Classical swine fever virus N^{pro} antagonises IRF3 to prevent IFN-independent TLR3 and RIG-I-mediated apoptosis

Samuel Hardy,[a,b] Ben Jackson,[a] Stephen Goodbourn,[b] Julian Seago[a]#

[a] The Pirbright Institute, Pirbright, Woking, Surrey, GU24 0NF, UK

[b] Institute for Infection and Immunity, St. George's, University of London, London, SW19 0RE, UK

Running title: CSFV N^{pro} antagonises IRF3-mediated apoptosis

Address correspondence to Julian Seago, julian.seago@pirbright.ac.uk

Abstract

Classical swine fever virus (CSFV) is the causative agent of classical swine fever, a notifiable disease of economic importance that causes severe leukopenia, fever and haemorrhagic disease in domesticated pigs and wild boar across the globe. CSFV has been shown to antagonise the induction of type I IFN, partly through a function of its N-terminal protease (N^{pro}) which binds IRF3 and targets it for proteasomal degradation. Additionally, N^{pro} has been shown to antagonise apoptosis triggered by the dsRNA-homolog poly(I:C), however the exact mechanism by which this is achieved has not been fully elucidated. In this study we confirm the ability of N^{pro} to inhibit dsRNA-mediated apoptosis and show that N^{pro} is also able to antagonise Sendai virus-mediated apoptosis in PK-15 cells. Gene edited PK-15 cell lines were used to show the dsRNA-sensing pathogen recognition receptors (PRRs) TLR3 and RIG-I specifically respond to poly(I:C) and SeV respectively, subsequently triggering apoptosis through pathways that converge on IRF3 and culminate in the cleavage of caspase-3. Importantly, this IRF3-mediated apoptosis was found to be dependent on transcription-independent functions of IRF3 and also on Bax, a pro-apoptotic Bcl-2 family protein, through a direct interaction between the two proteins. Deletion of IRF3, stable expression of N^{pro} and infection with wild-type CSFV were found to antagonise the mitochondrial localisation of Bax, a key hallmark of the intrinsic, mitochondrial pathway of apoptosis. Together, these findings show that N^{pro}'s putative interaction with IRF3 is involved not only in its antagonism of type I IFN, but also dsRNA-mediated mitochondrial apoptosis.

48 # Importance

49 Responsible for severe haemorrhagic disease in domestic pigs and wild boar, classical swine
50 fever is recognised by the World Organisation for Animal Health (OIE) and European Union as a
51 notifiable disease of economic importance. Persistent infection, immunotolerance and early
52 dissemination of the virus at local sites of infection have been linked to the antagonism of type I
53 IFN induction by N^{pro}. This protein may further contribute to these phenomena by antagonising
54 the induction of dsRNA-mediated apoptosis. Ultimately, apoptosis is an important innate
55 mechanism by which cells counter viruses at local sites of infection, thus preventing wider
56 spread and dissemination within the host, potentially also contributing to the onset of
57 persistence. Elucidation of the mechanism by which N^{pro} antagonises the apoptotic response
58 will help inform the development of rationally-designed live-attenuated vaccines and antivirals
59 for control of outbreaks in typically CSFV-free countries.

60

61

62

63

64

65

66

67

68 # Introduction

69 Classical swine fever virus (CSFV), a Pestivirus within the *Flaviviridae* family of positive-sense
70 RNA viruses, is the causative agent of classical swine fever (CSF), a notifiable disease of
71 domesticated pigs and wild boar. Recent and historic outbreaks have been associated with
72 significant economic losses and concurrently animal welfare is severely affected (1, 2). CSFV
73 virulence and clinical outcome is multifactorial, being both age and strain-dependent (3, 4).
74 Infection of piglets less than 12 weeks of age manifests as an acute disease associated with
75 severe leukopenia, fever, haemorrhagic disease and a host of neurological complications
76 (ataxia, convulsions) and death follows 1-3 weeks later. Disease is less acute in older pigs, often
77 resulting in chronic infection, a phenomenon also observed prenatally in piglets infected 50-70
78 days into gestation (5). Paradoxically, chronic and prenatal infection is always lethal while
79 recovery from acute infection is possible (2). Together, these observations suggest a complex
80 interplay between the virus and the host immune system.

81 As with IFN, apoptosis of infected cells ultimately serves as yet another mechanism by which
82 the intracellular innate immune system is able to counter the viruses at the local site of
83 infection and prevent their wider dissemination within the host (6). Leukopenia in CSFV-
84 infected pigs is thought to occur as a consequence of cell death (7, 8), however these cells
85 rarely contain virus (9). Taking into account the high titres of virus detected in acutely infected
86 pigs, infected cells resistant to virus-induced apoptosis likely have a role to play in determining
87 the overall clinical outcome (10, 11).

88 Apoptosis is an orderly programme of cell death employed by multicellular organisms to
89 eliminate damaged, aberrant or infected cells (12). Intracellular stimuli such as DNA damage
90 utilise a mitochondrial pathway of cell death regulated by Bcl-2 family proteins that serves to
91 trigger release of cytochrome c from the mitochondria into the cytosol (13). Subsequently,
92 cytochrome c associates with Apaf-1 to form a heptametric complex called the apoptosome,
93 enabling the cleavage of caspase-9 and the effector caspases 3 and 7 (14). Death receptor-
94 mediated cell death is triggered in response to death factor ligands of the TNF family (TNFα,
95 FasL, TRAIL). Upon ligand binding, a death-inducing signalling complex (DISC) is formed, cleaving
96 caspase-8 which can either cleave effector caspases directly or by cleaving Bid (tBid) to activate
97 mitochondrial apoptosis (15). Viral antagonism of apoptosis is well documented: African swine
98 fever virus A179L achieves this by directly binding tBid and Bax (16, 17) while vFLIP of γ-
99 herpesviruses prevents interaction of caspase-8 with the DISC (18). Homology of viral proteins
100 with host anti-apoptotic factors is often responsible for this antagonism.

101 The CSFV genome encodes four structural and seven non-structural proteins that are initially
102 translated as a single polyprotein (19). N^{pro}, a cysteine autoprotease, undergoes autocatalytic
103 cleavage from the polyprotein (20, 21) and has been demonstrated to interact with proteins in
104 order to modulate the intracellular innate immune response comprised primarily of type I
105 interferon (IFN-α/β) and apoptosis. N^{pro} interacts with interferon regulatory factor 3 (IRF3)
106 resulting in its proteasomal degradation and the elimination of host cell capacity to induce IFN
107 in response to the pathogen-associated molecular pattern (PAMP) dsRNA, a replication
108 intermediate of RNA viruses (22, 23). The ability of N^{pro} to antagonise dsRNA-mediated
109 apoptosis is, however, not well characterised and the mechanism remains to be properly

110 elucidated (24, 25). In addition, the pathways through which agonists such as dsRNA induce
111 apoptosis in porcine cell lines routinely used to study CSFV require examination.

112 Herein we confirm the ability of N^{pro} to inhibit dsRNA-mediated apoptosis and also show that
113 N^{pro} is able to antagonise Sendai virus-mediated apoptosis. Gene edited PK-15 cell lines were
114 used to show the dsRNA-sensing pathogen recognition receptors (PRRs) TLR3 and RIG-I
115 specifically mediated apoptotic responses to poly(I:C) and SeV respectively. We demonstrate
116 that CSFV N^{pro}'s interaction with porcine IRF3 is responsible not only for the antagonism of IFN
117 induction but also the innate apoptotic response and is mediated by an inhibition of the IRF3
118 dependent mitochondrial translocation of Bax, a pro-apoptotic Bcl-2 family protein.

119 # Results

120 ## N^{pro} antagonises poly(I:C) and Sendai virus-mediated apoptosis in PK-15 cells

121 To confirm previous reports of N^{pro}'s ability to antagonise dsRNA-mediated apoptosis, a porcine
122 kidney cell line (PK-15) stably expressing His-tagged N^{pro} was treated with poly(I:C) before
123 whole cell lysates were examined by Western blot for cleaved caspase-3, a terminal indicator of
124 apoptosis. As expected, Western blot analysis showed that caspase-3 was cleaved in parental
125 PK-15 cells treated with poly(I:C) (FIG 1A). In contrast, the His-N^{pro} cell line exhibited a
126 comparatively reduced level of cleaved caspase-3 following poly(:C) treatment, confirming
127 antagonism of the innate apoptotic response (FIG 1A). As expected for cell lines that showed
128 reduced levels of IRF3, the interferon stimulated genes (ISGs) Mx1, ISG15 and RIG-I were not
129 upregulated in N^{pro}-expressing lines following the treatment (FIG 1A). Poly(I:C) is thought to be
130 an agonist of TLR3-mediated signalling when added to cell culture media. The His-N^{pro} cell line
131 was next treated with Sendai virus (SeV, Cantell strain), a reported agonist of RIG-I-mediated
132 signalling. Similar to that observed for poly(I:C) treatment (FIG 1A), Western blot analysis of
133 whole cell lysates confirmed that SeV was able to induce the cleavage of caspase-3 in control
134 PK-15 cells, but comparatively lower levels of caspase-3 cleavage were observed for the His-N^{pro}
135 cell line (FIG 1A). Subsequent analyses of ISG levels in the respective whole cell lysates showed
136 that SeV treatment induced the expression of Mx1, ISG15 and RIG-I in the control PK-15 cells
137 and to a comparatively lower level in the His-N^{pro} cell line, demonstrating N^{pro}'s ability to
138 anatgonise SeV-induced ISG upregulation (FIG 1A).

139 Using lentivirus, we developed PK-15 cell lines stably expressing EGFP-tagged N^{pro} to further
140 validate these observations. Indeed, Western blot analyses of three individual cell lines
141 expressing EGFP-tagged N^{pro} confirmed their ability to anatagonise poly(I:C) and SeV-mediated
142 cleaved caspase-3 production and ISG upregulation in comparison to a control EGFP cell line
143 (FIG 1B).

144 As we have adopted cleaved caspase-3 as our primary readout for apoptosis, N^{pro} and CSFV
145 were assessed for their capacity to antagonise apoptosis mediated by staurosporine (STS), an
146 agonist which triggers caspase-3 cleavage through pathways independent of those typically
147 associated with dsRNA signalling (26, 27). In agreement with past observations (25), when
148 CSFV-infected PK-15 cells or a PK-15 cell line stably expressing His-N^{pro} were treated with STS,
149 levels of cleaved caspase-3 were comparable to that observed in uninfected control cells (FIG
150 1C).

151 Type I IFN amplifies poly(I:C)-mediated apoptosis in PK-15 and SK6 cells but is
152 not essential

153 Since we as well as others have observed N^{pro}'s clear antagonism of poly(I:C)-mediated IFN-
154 induction and ISG upregulation (22-24, 28), we wanted to establish whether IFN had any role in
155 the induction of apoptosis in response to each agonist – poly(I:C) and SeV. To do this, WT PK-15
156 cells were treated with either poly(I:C) or SeV in the presence of the JAK-STAT inhibitor
157 Ruxolitinib (RXT, FIG 2A) and whole cell lysates were then analysed by Western blot for cleaved
158 caspase-3. Interestingly, a large reduction in cleaved caspase-3 was observed in comparison to
159 cells treated with poly(I:C) in the absence of RXT (FIG 2B). However, the levels of cleaved

160 caspase-3 in cells treated with SeV were unaffected by the presence of RXT. To confim RXT
161 treatment had efficiently blocked IFN signalling following poly(I:C) treatment, lysates were then
162 analysed for the ISGs Mx1, ISG15 and RIG-I; as expected, the upregulation of Mx1 and RIG-I was
163 inhibited in the presence of RXT, while ISG15 upregulation was only partially antagonised since
164 IRF3 can bind directly to its promoter (29-31).

165 In order to further elucidate the impact that IFN has on poly(I:C)-mediated apoptosis, PK-15 and
166 SK6 cells were treated with poly(I:C) in the presence of increasing quantities of porcine IFN-α (0,
167 100, 1000 IU/ml). For both the PK-15 and SK6 treated cells, subsequent Western blot analyses
168 revealed a positive correlation between the quantity of IFN-α used and the observed level of
169 cleaved caspase-3 (FIG 2C). The increase in cleaved caspase-3 was most noticable with SK6 cells,
170 a cell line known to be incapable of producing endogenous type I IFN (28). Importantly, IFN-α
171 treatment alone was incapable of triggering levels of caspase-3 cleavage comparable to that
172 which was observed in cells treated with poly(I:C) alone.

173 Poly(I:C) and SeV-mediated apoptosis is dependent on TLR3 and RIG-I signalling
174 pathways converging on IRF3 in PK-15 cells

175 In order to identify the innate cell signalling pathways through which poly(I:C) and SeV induce
176 apoptosis in PK-15 cells, and to help elucidate the mechanism that N^{pro} uses to achieve the
177 observed antagonism of apoptosis, PK-15 cell lines were developed that had been gene edited
178 to knockout the expression of TLR3 ($TLR3^{-/-}$) and RIG-I ($RIG\text{-}I^{-/-}$). For each targeted gene,
179 individual cell lines were generated and validated by PCR, sequencing and, when a suitable
180 antibody was available, by Western blot. Each cell line was screened by Western blot for

181 responsiveness to poly(I:C) and SeV in the presence or absence of RXT. Cleaved caspase-3 was
182 undetectable in TLR3$^{-/-}$ cells following poly(I:C) treatment, whereas the cleavage of caspase-3
183 induced by SeV infection was unaffected by the loss of TLR3 (FIG 3A, 3B). In contrast, RIG-I$^{-/-}$ cell
184 lines displayed the opposite phenotype, namely loss of cleavage of capsase-3 in response to
185 SeV but normal cleavage in response to poly(I:C) (FIG 3C, 3D). These results confirmed that
186 poly(I:C) and SeV trigger apoptosis in PK-15 cells specifically via TLR-3 and RIG-I, respectively.

187 Since TLR3 and RIG-I signalling pathways are classically known to converge on IRF3 to activate
188 the IFN-β promoter, we next investigated if IRF3 is also required for the induction of apoptosis.
189 To facilitate this, PK-15 cell lines gene edited to knockout IRF3 (IRF3$^{-/-}$) were prepared and
190 validated (manuscript submitted for publication, Jackson *et al*. 2020). Interestingly, no cleaved
191 caspase-3 was observed when IRF3$^{-/-}$ PK-15 cells were treated with either poly(I:C) or SeV (FIG
192 3E, 3F). In each case, absence of caspase-3 cleavage was associated with an absence of ISG
193 upregulation, highlighting that the pathways responsible for IFN induction are also responsible
194 for induction of the innate apoptotic response to these antagonists. The presence of RXT had
195 no observable effect on caspase-3 cleavage in the knockout PK-15 cell lines.

196 Bax directly mediates apoptosis in a manner that depends upon transcription-
197 independent functions of IRF3

198 Having shown that IRF3 is required for the induction of TLR3 and RIG-I-mediated apoptotic
199 responses, it was important to determine the mechanism of IRF3 function. IRF3 has been
200 reported to play a role in a transcription-independent pathway of apoptosis that relies upon an
201 interaction with the pro-apoptotic protein Bax and its subsequent translocation to the

202 mitochondrial membrane in murine and human cells (32-34). To establish whether porcine IRF3
203 interacts with porcine Bax, the yeast two-hybrid (Y-2-H) system was employed. In agreement
204 with previous reports (35-37), we found full-length Bax expression toxic in yeast, but a
205 truncated mutant lacking the C-terminus transmembrane domain (BaxΔC) exhibited less toxicity
206 (38-40) and was used to successfully confirm the interaction (FIG 4A). Further Y-2-H analyses
207 confirmed $N^{pro'}$s ability to interact with porcine IRF-3, but no direct interaction between N^{pro}
208 and BaxΔC was observed (FIG 4A). To validate the physiological significance of this interaction,
209 additional PK-15 cell lines were developed that had been gene edited to knockout the
210 expression of Bax ($Bax^{-/-}$); successful knockout was confirmed by Western blot. Subsequently,
211 $Bax^{-/-}$ cells were screened by live-cell bright-field microscopy (FIG 4B) and Western blot (FIG 4C)
212 for their responsiveness to poly(I:C) and SeV, identified as specific ligands for TLR3 and RIG-I
213 respectively in PK-15 cells (FIG 3). Unedited PK-15 cells displayed significant rounding and
214 detachment following both poly(I:C) and SeV treatment, indicative of apoptosis. In contrast,
215 $Bax^{-/-}$ PK-15 cells remained largely unchanged following each treatment (FIG 4B). Cleaved
216 caspase-3 was undetectable in $Bax^{-/-}$ cells following each treatment while Mx1 and ISG15 were
217 detected at comparable levels in both unedited and $Bax^{-/-}$ PK-15 cells (FIG 4C). These results
218 confirmed that IRF3-mediated apoptosis is Bax-dependent.

219 IRF3 is best known for its function as a transcription factor, mediating the upregulation of not
220 only type I IFN but also a small subset of “IFN-independent” ISGs (29-31). In order to determine
221 whether apoptosis requires IRF3 transcriptional activity, $IRF3^{-/-}$ PK-15 cells stably expressing a
222 FLAG-tagged transcriptionally inactive IRF3 mutant termed “S1” (S394A, S396A) (32, 41) were
223 generated using lentivirus (FIG 4D). These serine residues are potentially required for the

224 interaction between IRF3 and CREB-binding protein (CBP), a prerequisite for the binding of IRF3
225 to gene promoters (42-44), and are also highly conserved across multiple species (FIG 4D). In
226 mice, the S1 mutations eliminate the ability of IRF3 to stimulate transcription while preserving
227 its pro-apoptotic functions (32). As a control, an IRF3$^{-/-}$ PK-15 cell line stably expressing FLAG-
228 tagged WT IRF3 was also generated. Both cell lines were then subjected to poly(I:C) treatment
229 and whole cell lysates were examined by Western blot for the presence of Mx1 as an indicator
230 of IRF3 transcriptional activity, as well as cleaved caspase-3 to determine the induction of
231 apoptosis. Mx1 was undetectable in S1 samples following poly(I:C) treatment, confirming the
232 loss of transcriptional activity and ability to induce type I IFN. In contrast, Mx1 was observed in
233 the corresponding WT samples. However, cleaved caspase-3 was observed in both the WT and
234 to a lesser extent the S1 IRF3 samples (FIG 4E), confirming that the transcriptionally inactive S1
235 mutant could still mediate apoptosis. Similar experiments using SeV treatment led to
236 comparable levels of caspase-3 cleavage (FIG 4E) in WT and S1 IRF3-expressing IRF3$^{-/-}$ PK-15 cell
237 lines. Together, these results confirmed that IRF3 mediates a Bax-dependent pathway of
238 apoptosis, even when devoid of its ability to act as a transcription factor.

239 N^{pro} blocks poly(I:C) and Sendai virus-mediated mitochondrial localisation of Bax

240 In the present work, IRF3 has been shown to coordinate a TLR3 and RIG-I-mediated Bax-
241 dependent pathway of apoptosis independent of its activity as a transcription factor, supporting
242 previous observations made by Chattopadhyay *et al.* (32-34). However, the exact nature of
243 porcine Bax's role in this process remains to be determined. CSFV N^{pro} has previously been
244 shown to antagonise poly(I:C)-mediated mitochondrial release of cytochrome c and caspase-9
245 cleavage (25). Furthermore, N^{pro}'s ability to target IRF3 for ubiquitin-dependent proteasomal

246 degradation has been well documented (22). We therefore decided to investigate if Bax can
247 localise to the mitochondrial membrane following the induction of apoptosis in the presence of
248 N^{pro} and in the absence of IRF3.

249 Experiments using PK-15 cells and immunofluorescence confocal microscopy were performed
250 to confirm the localisation of endogenous Bax to the mitochondria following exposure to the
251 agonists poly(I:C) or SeV. In both poly(I:C) or SeV-treated PK-15 cells Bax localisation was
252 undetectable prior to treatment, in agreement with published literature (32-34). However,
253 following treatment with either poly(I:C) or SeV, Bax was detectable, appearing as distinct,
254 condensed puncta that co-localised with the mitochondrial membrane, but did not appear to
255 have been internalised (FIG 5A, 5B). In PK-15 cells that had been treated with either agonist the
256 mitochondria exhibited a condensed morphology characteristic of apoptosis. Bax localistaion
257 was also investigated in PK-15 cell lines stably expressing N^{pro} and in the PK-15 $IRF3^{-/-}$ cell lines.
258 While a large proportion of WT PK-15 cells displayed mitochondrial localisation of Bax, there
259 was a complete absence in both the N^{pro} and $IRF3^{-/-}$ PK-15 cell lines tested (FIG 5A). These
260 experiments were performed in the presence of Z-VAD(OMe)-FMK (Bachem), an inhibitor of the
261 effector caspases, in order to maximise the number of cells for visualisation by
262 immunofluorescence following treatment with each apoptosis agonist. Collectively, these
263 observations highlight the role of Bax in IRF3-medated apoptosis and confirm its antagonism by
264 N^{pro}.

265 Having shown that the presence of N^{pro} inhibited the mitochondrial localisation of Bax,
266 experiments were conducted to determine whether N^{pro} can also modulate Bax expression in a
267 similar manner to that observed for IRF3. Western blot analysis of whole cell lysates prepared

268 from untreated WT and N^{pro}-expressing PK-15 cells indicated that Bax is not targeted by N^{pro} for
269 degradation (FIG 5C). Interestingly, poly(I:C) treatment led to an increase in the level of N^{pro}
270 protein compared to untreated cells, raising a possibility of stabilisation in the presence of a
271 target protein.

272 Antagonism of SeV-mediated apoptosis in CSFV-infected cells is dependent on
273 the expression of N^{pro}

274 In order to investigate whether CSFV infection has the same antagonistic effect on apoptosis as
275 stably-expressed N^{pro}, SK6 cells were infected (MOI of 0.2) with either CSFV Alfort, CSFV Brescia,
276 a recombinant CSFV (rCSFV) Alfort or an N^{pro}-deleted (ΔN^{pro}) rCSFV Alfort; infections were
277 allowed to continue until most cells had been infected (as determined by CSFV E2 expression).
278 Infected cells were then treated with SeV prior to analysis by immunofluorescence microscopy
279 (FIG 6A). Due to the inability of ΔN^{pro} rCSFV Alfort to efficiently replicate in PK-15 cells (28), SK6
280 cells were instead used as they lack the capacity to produce type I IFN and are sensitive to
281 dsRNA-mediated apoptosis (24, 28). The SK6 cells that were infected with either CSFV Alfort,
282 CSFV Brescia or rCSFV Alfort prior to SeV treatment displayed significantly reduced Bax
283 localisation to the mitochondria ($p<.001$), however those infected with ΔN^{pro} rCSFV Alfort
284 displayed levels of localisation comparable to uninfected control cells (FIG 6A, 6B). CSFV was
285 not assessed for its capacity to antagonise poly(I:C)-mediated apoptosis as the ΔN^{pro} virus still
286 encodes the soluble and secretable endoribonuclease E^{rns} which acts as a scavenger receptor
287 for dsRNA (45, 46); a double mutant ΔN^{pro} ΔE^{rns} virus was unavailable.

288 We subsequently infected (MOI of 0.2) PK-15 cells with either CSFV Alfort or CSFV Brescia in
289 order to validate the capacity of CSFV infection to antagonise induction of apoptosis in a more
290 relevant, IFN-competent cell line. As with the SK6 infections, PK-15 cells infected with either
291 CSFV Alfort or CSFV Brescia displayed reduced Bax localisation to the mitochondria ($p<.001$)
292 (FIG 6A, 6C). In summary, these results confirm that CSFV is indeed capable of antagonising
293 SeV-mediated mitochondrial Bax localisation in multiple porcine kidney endothelial cell lines,
294 suggesting a clear capacity to antagonise induction of apoptosis dependent on the expression
295 of N^{pro}.

296 Discussion

297 Generated as replication intermediates of the RNA virus genome, dsRNA triggers the induction
298 of innate responses such as type I IFN and apoptosis. The apoptosis triggered by dsRNA as a
299 consequence of infection is thought to have a protective role, serving to limit further virus
300 dissemination within the host (6). When expressed stably and during infection, CSFV N^{pro} has
301 been shown to antagonise both of these responses (22-25, 28). While N^{pro}'s putative interaction
302 with IRF3 has been identified as the source of IFN antagonism, the mechanism by which N^{pro}
303 antagonises the induction of dsRNA-meditated apoptosis has yet to be identified. Using a
304 combination of CRISPR-Cas9 gene-editing technology and confocal microscopy, we report that
305 in porcine kidney endothelial cells IRF3 coordinates the induction of RIG-I and TLR3-mediated
306 apoptosis in an IRF3-dependent IFN-independent manner, culminating in the localisation of pro-
307 apoptotic Bax to the mitochondrial membrane and induction of caspase-3 cleavage, a key
308 hallmark of apoptosis.

309 Initially we identified the pathways that N^{pro} is able to antagonise and thereafter identified the
310 PRRs through which agonists were sensed in order to elucidate the mechanism of apoptosis
311 inhibition used by N^{pro}. In addition to antagonising apoptosis mediated by poly(I:C), a reported
312 TLR3 agonist and dsRNA homolog, we report that N^{pro} expressed stably in cell culture and
313 during infection can also antagonise SeV-mediated apoptosis. This finding was interesting since
314 SeV copy-back defective interfering (cbDI) RNA is widely reported to be an agonist of the RIG-I
315 signalling pathway (47-49) and showed that N^{pro} is capable of targeting pro-apoptotic signalling
316 triggered by multiple pathways. CRISPR-Cas9 knockouts of both TLR3 and RIG-I subsequently
317 confirmed them to be essential in PK-15 cells for the induction of caspase-3 cleavage in
318 response to poly(I:C) and SeV respectively and found IRF3 to be indispensable in each case.

319 Since N^{pro}'s putative interaction with IRF3 and its consequent antagonism of type I IFN
320 induction are well published, we intended to determine whether IFN has any role in the
321 caspase-3 cleavage observed in response to TLR3 and RIG-I agonists poly(I:C) and SeV.
322 Pharmacological inhibition of the JAK-STAT pathway using RXT and subsequent treatment of
323 cells with porcine IFN-α revealed the apoptosis mediated by poly(I:C), but not SeV, to be
324 amplified while IFN-α alone appeared to cause no detectable caspase-3 cleavage. The type I IFN
325 response is required for the upregulation of a diverse range of ISGs, a number of which are pro-
326 apoptotic. In light of this, it is possible that components of the TLR3 signalling pathway might be
327 upregulated by type I IFN, thus explaining the observed amplification of caspase-3 cleavage.
328 Shaw *et al.* reported upregulation of TLR3, caspase-8, Noxa and TRAIL expression in *ex vivo*
329 porcine skin fibroblast cultures following IFN treatment (50) while Renson *et al.* found elements
330 of the Fas and TRAIL signalling pathways to be upregulated in uninfected bystander peripheral

331 blood mononuclear cells (PBMC) during *in vivo* infection with a related Pestivirus, BVDV (51).
332 Direct amplification of poly(I:C)-mediated apoptosis by IFN-α has also been described (52),
333 however the capacity of each to modulate the innate apoptotic response likely varies
334 depending on tissue and cell type. SeV encodes C-protein, an antagonist of STAT1
335 phosphorylation, which likely explains the apparent absence of ISG upregulation or subsequent
336 effect from the RXT treatment (53).

337 The apparent importance of IRF3 in coordinating the induction of pro-apoptotic TLR3 and RIG-I
338 mediated responses proved insightful since IRF3 has previously been implicated in the induction
339 of a dsRNA-mediated IRF3/Bax dependent pathway of apoptosis termed RIPA (RLR-induced
340 IRF3 mediated Pathway of Apoptosis) that also culminates in cleavage of caspase-3 (32-34).
341 Through a putative BH3-like domain, IRF3 has been shown to mediate its pro-apoptotic activity
342 through a direct interaction with Bax, facilitating its localisation to the mitochondrial membrane
343 (33). In this study, we have confirmed the interaction of porcine IRF3 and Bax using the Y-2-H
344 system, corroborating past observations (33). We have also shown that the aforementioned
345 IRF3/Bax dependent pathway of apoptosis is active in porcine kidney endothelial cells and
346 shown that IRF3-mediated apoptosis is dependent on the presence of Bax and does not require
347 IRF3's activity as a transcription factor. Importantly, apoptosis was actively antagonised by both
348 stable expression of N^{pro} and infection with CSFV as seen by the absence of, or significant
349 reduction in, mitochondrial Bax localisation and associated cleavage of caspase-3. Bax staining
350 in apoptotic cells appeared as distinct puncta associated with the mitochondria, likely
351 corresponding to the formation of homodimeric pores in the mitochondrial outer membrane
352 (MOM) (54-58) which have been reported to facilitate release of cytochrome c from the

353 intermembrane space (IMS) (59, 60). This is in agreement with a past study which found CSFV
354 to antagonise cytochrome c release and caspase-9 cleavage (25). Importantly, this localisation
355 occurred in a manner independent of Bax expression levels, lending further credence to the
356 idea that the observed phenotype is due to IFN-independent IRF3/Bax activity.

357 Jefferson *et al*. observed that transfected CSFV N^{pro} and the related Pestivirus BVDV
358 antagonised sodium arsenate-mediated mitochondrial Bax localisation (61). However, this
359 agonist is thought to trigger apoptosis by upregulating Bax expression in a c-Jun N-terminal
360 kinase (JNK)-dependent manner (62). Our study explored this pathway in the context of stably-
361 expressed N^{pro} and CSFV infection utilising authentic agonists of dsRNA signalling pathways. We
362 have demonstrated both poly(I:C) and SeV to be relevant and authentic agonists of TLR3 and
363 RIG-I signalling pathways that converge on IRF3 in their induction of apoptosis. The significance
364 of TLR3 and RIG-I mediated responses during CSFV infection was highlighted by Hüsser *et al*.
365 using shRNA knockdown to target each (63). No observable differences in ΔN^{pro} rCSFV growth
366 were observed in a representative $Bax^{-/-}$ cell line in comparison to wild-type cells (data not
367 shown). We suspect any differences were masked by the transcriptional activity of IRF3 and
368 subsequent ISG expression.

369 Taken together, these results suggest that N^{pro}'s interaction with IRF3 is not only responsible for
370 antagonising the induction of type I IFN but also the induction of IFN-independent IRF3/Bax-
371 mediated caspase-3 cleavage and apoptosis. Ultimately, N^{pro}'s antagonism of TLR3, RIG-I and
372 IRF3-mediated apoptotic responses serves as another mechanism of CSFV immune evasion,
373 likely contributing to the establishment of infection and host persistence.

374 # Materials and methods

375 ## Cell culture and viruses

376 All cells were maintained at 37°C in 5 % CO_2. PK-15, SK6 and HEK 293-T cell lines (obtained in-
377 house) were maintained in Dulbecco's Modified Eagle Medium (DMEM; Thermo Fisher), 5%
378 adult bovine serum (ABS; Selborne) demonstrated to be BVDV-free and anti-BVDV antibody
379 free, GlutaMAX (Thermo Fisher) and penicillin-streptomycin (50 IU/ml penicillin, 50 µg/ml
380 streptomycin, Thermo Fisher). CSFV-strains Alfort 187 and Brescia were kindly provided by the
381 EU reference laboratory (Hannover, Germany). The parental infectious clone EP#98/2 derived
382 from CSFV-strain Alfort Tübingen and the corresponding N^{pro}-deleted infectious clone EP#96/2
383 were a kind gift from Prof Gregor Meyers (FLI; Tübingen, Germany). Virus was grown in SK6
384 cells and isolated from washed cell pellets by freeze-thaw lysis. Immunostaining with anti-CSFV
385 E2 antibody WH303 (APHA) (64) was used to titre viruses by $TCID_{50}$ in SK6 cells and used in
386 experiments at a MOI of 0.2. Where indicated, cells were treated with inhibitor of JAK1/2
387 phosphorylation ruxolitinib (RXT; Selleckchem), recombinant porcine IFN-α (R&D Systems),
388 staurosporine (STS; Sigma), Sendai virus (SeV) Cantell strain (Charles River) and
389 polyinosinic:polycytidylic acid (poly(I:C); Sigma). Cells were treated with 0.5 µM RXT, 2.5 µM
390 STS, 100 µg/ml poly(I:C) and 200 HA/ml SeV except where stated otherwise.

391 ## Generation of cell lines stabling expressing recombinant proteins using
392 ## lentivirus

393 CSFV Alfort 187 cDNA was cloned into the 3rd-generation lentiviral vector pLJM1-EGFP, a gift
394 from David Sabatini (Addgene plasmid #19319) (65), to generate pLJM1-EGFP-N^{pro}. WT and S1

395 mutant (S396A, S398A) porcine IRF3 cDNAs bearing an N-terminal FLAG tag were cloned into a
396 modified pLJM1 vector devoid of EGFP to generate pLJM1-FLAG-IRF3 and pLJM1-FLAG-IRF3-S1.
397 Packaging plasmids (pLP1, pLP2, pLP/VSV-G) were co-transfected into HEK-293T cells a single
398 pLJM1 vector to generate EGFP, EGFP-N^{pro}, WT IRF3 and S1 IRF3 encoding lentiviruses
399 respectively. Lentiviruses were added to a low-passage PK-15 cell culture in the presence of 2
400 µg/ml polybrene (Sigma) and centrifuged at 1000 rcf for 30 min. 72 hours post-infection, cells
401 were treated for a further 72 hr with 3 µg/ml puromycin (Thermo Fisher) to select for
402 transduced cells. 48 hr after removal of selection, colonies of surviving cells were picked and
403 isolated for screening and validation.

404 **Generation of CRISPR-Cas9 knockout cell lines**

405 Guide RNAs (sgRNAs) were designed using the E-CRISP tool (http://www.e-crisp.org/E-
406 CRISP/designcrispr.html; German Cancer Research Center) and cloned into pSpCas9n(BB)-2A-
407 GFP (PX461) and pSpCas9n(BB)-2A-Puro (PX462) V2.0 plasmids encoding the D10A nickase
408 mutant of *S. pyogenes* Cas9 (Cas9n) baring puromycin and GFP selection markers respectively
409 (66). These plasmids were a gift from Feng Zhang (Addgene plasmids #48140 and #62987) (66).
410 $CaCl_2$-competent JM109 *E. coli* were transformed with each plasmid which was then extracted
411 and purified using a QIAprep Spin Miniprep Kit (Qiagen). Low-passage PK-15 cells were co-
412 transfected with each plasmid for 48 hr and 3 µg/ml puromycin selection (Thermo Fisher)
413 applied for a further 72 hr. 48 hr after removal of selection, colonies of surviving cells were
414 picked and isolated for screening and validation.

415

416 ## Western blot analysis

417 Proteins were separated by SDS-PAGE (4-20% polyacrylamide; Thermo Fisher) and transferred
418 to Amersham Protran 0.45 µm nitrocellulose membranes. Membranes were blocked with 5 %
419 (w/v) dried skimmed milk in PBS containing 0.5 % Tween-20. Anti-CSFV N^{pro} rabbit sera (DS14)
420 was generated in-house by inoculating rabbits with the peptide
421 KTNKQKPMGVEEPVYDATGKPLFGDPS corresponding to N-terminal residues 11-37 (67). Primary
422 mAbs recognising γ-tubulin (T6557; Sigma), Mx1 (Ab79609; Abcam), RIG-I (sc-376845; Santa
423 Cruz Biotechnology), CSFV E2 (WH303, APHA), and polyclonal Abs recognising ISG15 (sc-50366;
424 Santa Cruz Biotechnology), Bax (2772; Cell Signalling Technology), cleaved caspase-3 (9664; Cell
425 Signalling Technology), GFP (Ab290; Abcam) and FLAG (R1180; Acris) were all used as indicated.
426 Bound primary antibodies were detected by horseradish peroxidase-conjugated goat anti-
427 mouse (Promega) or goat anti-rabbit (Promega) secondary antibodies.

428 ## Immunofluorescence

429 Cells were prepared on coverglasses prior to treatments and fixed with 4 % paraformaldehyde
430 (Santa Cruz Biotechnology) for 1 hr, permeabilised with 0.1 % Triton X-100 for 5 min and
431 blocked in 10% goat serum [DETAILS] in PBSa (lacking $MgCl_2$ and $CaCl_2$). mAb recognising CSFV
432 E2 (WH303; APHA) and rabbit polyclonal Ab recognising Bax (2772; Cell Signalling Technology)
433 primary antibodies were used where indicated. Secondary antibodies were goat anti-mouse
434 Alexa Fluor 488 or 633-conjugated (Thermo Fisher). Nuclei were stained with DAPI (Sigma). For
435 mitochondrial staining, 150 nM MitoTracker red CMXRos (Thermo Fisher) diluted in complete
436 growth medium was added to the cells 30 min prior to washing in PBS and fixation. Prepared

437 slides of cells were imaged on a Leica TCS SP2Acousto-Optical Beam Splitter confocal scanning
438 laser microscope at wavelengths appropriate for each Alexa Fluor probe.

439 Where specified, protein localisation was quantified as follows: images were imported into
440 ImageJ and automated counting used to determine the total number of nuclei per field of view.
441 For Bax studies, cells demonstrating condensed mitochondrial localisation were manually
442 counted and divided by the nuclei count to give percentage positives. 2-way ANNOVA
443 (Graphpad) was used to determine mean, SD and CI for n=5.

444 Yeast two-hybrid analysis

445 The Matchmaker© 3 GAL4-based yeast two-hybrid system (Clontech Laboratories) was
446 employed to identify direct protein-protein interactions. A cDNA encoding CSFV N^{pro} (Alfort)
447 was cloned into the pGBKT7 and pGADT7 vectors to generate fusions with the GAL4 DNA-
448 binding and activation domains respectively. A cDNA encoding porcine IRF3 (NM_213770.1)
449 was additionally cloned into pGADT7 while a cDNA encoding porcine Bax (XM_003127290.5),
450 modified by PCR to lack the terminal 20 amino acids (Val^{173}-Gly^{192}), was cloned into each vector.
451 Yeast (AH109) were grown, maintained and transformed as instructed by the manufacturer
452 (Clontech Laboratories). Co-transformed yeast cultures were subsequently plated onto double-
453 dropout media deficient of leucine and tryptophan and quadruple-dropout media additionally
454 lacking adenine and histidine.

455 Acknowledgments

456 This work was supported by grants funded by the Biotechnology and Biological Sciences
457 Research Council (BBSRC), BBS/E/I/00007032 and BBS/E/I/00007037.

References

1. Meuwissen MP, Horst SH, Huirne RB, Dijkhuizen AA. 1999. A model to estimate the financial consequences of classical swine fever outbreaks: principles and outcomes. Prev Vet Med 42:249-70.
2. Moennig V, Floegel-Niesmann G, Greiser-Wilke I. 2003. Clinical Signs and Epidemiology of Classical Swine Fever: A Review of New Knowledge. The Veterinary Journal 165:11-20.
3. Floegel-Niesmann G, Bunzenthal C, Fischer S, Moennig V. 2003. Virulence of recent and former classical swine fever virus isolates evaluated by their clinical and pathological signs. J Vet Med B Infect Dis Vet Public Health 50:214-20.
4. Moennig V, Floegel-Niesmann G, Greiser-Wilke I. 2003. Clinical signs and epidemiology of classical swine fever: a review of new knowledge. Vet J 165:11-20.

481 5. Munoz-Gonzalez S, Ruggli N, Rosell R, Perez LJ, Frias-Leuporeau MT, Fraile L, Montoya M,
482 Cordoba L, Domingo M, Ehrensperger F, Summerfield A, Ganges L. 2015. Postnatal persistent
483 infection with classical Swine Fever virus and its immunological implications. PLoS One
484 10:e0125692.
485 6. Jorgensen I, Rayamajhi M, Miao EA. 2017. Programmed cell death as a defence against infection.
486 Nature reviews Immunology 17:151-164.
487 7. Choi C, Hwang KK, Chae C. 2004. Classical swine fever virus induces tumor necrosis factor-alpha
488 and lymphocyte apoptosis. Arch Virol 149:875-89.
489 8. Sanchez-Cordon PJ, Romanini S, Salguero FJ, Nunez A, Bautista MJ, Jover A, Gomez-Villamos JC.
490 2002. Apoptosis of thymocytes related to cytokine expression in experimental classical swine
491 fever. J Comp Pathol 127:239-48.
492 9. Summerfield A, Knoetig SM, Tschudin R, McCullough KC. 2000. Pathogenesis of
493 Granulocytopenia and Bone Marrow Atrophy during Classical Swine Fever Involves Apoptosis
494 and Necrosis of Uninfected Cells. Virology 272:50-60.
495 10. Tamura T, Nagashima N, Ruggli N, Summerfield A, Kida H, Sakoda Y. 2014. Npro of classical
496 swine fever virus contributes to pathogenicity in pigs by preventing type I interferon induction at
497 local replication sites. Vet Res 45:47.
498 11. Summerfield A, Ruggli N. 2015. Immune responses against classical swine fever virus: between
499 ignorance and lunacy. Frontiers in Veterinary Science 2.
500 12. Nagata S. 2018. Apoptosis and Clearance of Apoptotic Cells. 36:489-517.
501 13. Czabotar PE, Lessene G, Strasser A, Adams JM. 2014. Control of apoptosis by the BCL-2 protein
502 family: implications for physiology and therapy. Nat Rev Mol Cell Biol 15:49-63.
503 14. Srinivasula SM, Ahmad M, Fernandes-Alnemri T, Alnemri ES. 1998. Autoactivation of
504 procaspase-9 by Apaf-1-mediated oligomerization. Mol Cell 1:949-57.
505 15. Strasser A, Jost PJ, Nagata S. 2009. The many roles of FAS receptor signaling in the immune
506 system. Immunity 30:180-92.
507 16. Banjara S, Caria S, Dixon LK, Hinds MG, Kvansakul M. 2017. Structural Insight into African Swine
508 Fever Virus A179L-Mediated Inhibition of Apoptosis. Journal of virology 91:e02228-16.
509 17. Galindo I, Hernaez B, Diaz-Gil G, Escribano JM, Alonso C. 2008. A179L, a viral Bcl-2 homologue,
510 targets the core Bcl-2 apoptotic machinery and its upstream BH3 activators with selective
511 binding restrictions for Bid and Noxa. Virology 375:561-72.
512 18. Glykofrydes D, Niphuis H, Kuhn EM, Rosenwirth B, Heeney JL, Bruder J, Niedobitek G, Müller-
513 Fleckenstein I, Fleckenstein B, Ensser A. 2000. Herpesvirus saimiri vFLIP provides an
514 antiapoptotic function but is not essential for viral replication, transformation, or pathogenicity.
515 Journal of virology 74:11919-11927.
516 19. Lindenbach B, Thiel HJ, Rice CM. 2007. Flaviviridae: The viruses and their replication. Fields
517 Virology:1101-1151.
518 20. Stark R, Meyers G, Rümenapf T, Thiel HJ. 1993. Processing of pestivirus polyprotein: cleavage
519 site between autoprotease and nucleocapsid protein of classical swine fever virus. Journal of
520 Virology 67:7088-7095.
521 21. Rumenapf T, Stark R, Heimann M, Thiel HJ. 1998. N-terminal protease of pestiviruses:
522 identification of putative catalytic residues by site-directed mutagenesis. J Virol 72:2544-7.
523 22. Seago J, Hilton L, Reid E, Doceul V, Jeyatheesan J, Moganeradj K, McCauley J, Charleston B,
524 Goodbourn S. 2007. The Npro product of classical swine fever virus and bovine viral diarrhea
525 virus uses a conserved mechanism to target interferon regulatory factor-3. J Gen Virol 88:3002-
526 6.

527 23. Bauhofer O, Summerfield A, Sakoda Y, Tratschin J-D, Hofmann MA, Ruggli N. 2007. Classical
528 Swine Fever Virus N(pro) Interacts with Interferon Regulatory Factor 3 and Induces Its
529 Proteasomal Degradation. Journal of Virology 81:3087-3096.
530 24. Ruggli N, Bird BH, Liu L, Bauhofer O, Tratschin J-D, Hofmann MA. 2005. Npro of classical swine
531 fever virus is an antagonist of double-stranded RNA-mediated apoptosis and IFN-α/β induction.
532 Virology 340:265-276.
533 25. Johns HL, Bensaude E, La Rocca SA, Seago J, Charleston B, Steinbach F, Drew TW, Crooke H,
534 Everett H. 2010. Classical swine fever virus infection protects aortic endothelial cells from pIpC-
535 mediated apoptosis. J Gen Virol 91:1038-46.
536 26. Belmokhtar CA, Hillion J, Segal-Bendirdjian E. 2001. Staurosporine induces apoptosis through
537 both caspase-dependent and caspase-independent mechanisms. Oncogene 20:3354-62.
538 27. Zhang XD, Gillespie SK, Hersey P. 2004. Staurosporine induces apoptosis of melanoma by both
539 caspase-dependent and -independent apoptotic pathways. Molecular Cancer Therapeutics
540 3:187-197.
541 28. Ruggli N, Tratschin JD, Schweizer M, McCullough KC, Hofmann MA, Summerfield A. 2003.
542 Classical swine fever virus interferes with cellular antiviral defense: evidence for a novel function
543 of N(pro). J Virol 77:7645-54.
544 29. Memet S, Besancon F, Bourgeade MF, Thang MN. 1991. Direct induction of interferon-gamma-
545 and interferon-alpha/beta-inducible genes by double-stranded RNA. J Interferon Res 11:131-41.
546 30. Daly C, Reich NC. 1995. Characterization of specific DNA-binding factors activated by double-
547 stranded RNA as positive regulators of interferon alpha/beta-stimulated genes. J Biol Chem
548 270:23739-46.
549 31. Ashley CL, Abendroth A, McSharry BP, Slobedman B. 2019. Interferon-Independent Upregulation
550 of Interferon-Stimulated Genes during Human Cytomegalovirus Infection is Dependent on IRF3
551 Expression. Viruses 11:246.
552 32. Chattopadhyay S, Kuzmanovic T, Zhang Y, Wetzel JL, Sen GC. 2016. Ubiquitination of the
553 Transcription Factor IRF-3 Activates RIPA, the Apoptotic Pathway that Protects Mice from Viral
554 Pathogenesis. Immunity 44:1151-61.
555 33. Chattopadhyay S, Marques JT, Yamashita M, Peters KL, Smith K, Desai A, Williams BRG, Sen GC.
556 2010. Viral apoptosis is induced by IRF-3-mediated activation of Bax. The EMBO Journal 29:1762-
557 1773.
558 34. Chattopadhyay S, Yamashita M, Zhang Y, Sen GC. 2011. The IRF-3/Bax-mediated apoptotic
559 pathway, activated by viral cytoplasmic RNA and DNA, inhibits virus replication. J Virol 85:3708-
560 16.
561 35. Sato T, Hanada M, Bodrug S, Irie S, Iwama N, Boise LH, Thompson CB, Golemis E, Fong L, Wang
562 HG. 1994. Interactions among members of the Bcl-2 protein family analyzed with a yeast two-
563 hybrid system. Proceedings of the National Academy of Sciences of the United States of America
564 91:9238-9242.
565 36. Hanada M, Aimé-Sempé C, Sato T, Reed JC. 1995. Structure-function analysis of Bcl-2 protein.
566 Identification of conserved domains important for homodimerization with Bcl-2 and
567 heterodimerization with Bax. J Biol Chem 270:11962-9.
568 37. Greenhalf W, Stephan C, Chaudhuri B. 1996. Role of mitochondria and C-terminal membrane
569 anchor of Bcl-2 in Bax induced growth arrest and mortality in Saccharomyces cerevisiae. FEBS
570 Lett 380:169-75.
571 38. Zha H, Fisk HA, Yaffe MP, Mahajan N, Herman B, Reed JC. 1996. Structure-function comparisons
572 of the proapoptotic protein Bax in yeast and mammalian cells. Molecular and Cellular Biology
573 16:6494.

574 39. Schinzel A, Kaufmann T, Schuler M, Martinalbo J, Grubb D, Borner C. 2004. Conformational
575 control of Bax localization and apoptotic activity by Pro168. The Journal of cell biology 164:1021-
576 1032.
577 40. Nechushtan A, Smith CL, Hsu YT, Youle RJ. 1999. Conformation of the Bax C-terminus regulates
578 subcellular location and cell death. Embo j 18:2330-41.
579 41. Sanz-Garcia C, McMullen MR, Chattopadhyay S, Roychowdhury S, Sen G, Nagy LE. 2019.
580 Nontranscriptional Activity of Interferon Regulatory Factor 3 Protects Mice From High-Fat Diet-
581 Induced Liver Injury. Hepatology Communications 3:1626-1641.
582 42. Lin R, Heylbroeck C, Pitha PM, Hiscott J. 1998. Virus-dependent phosphorylation of the IRF-3
583 transcription factor regulates nuclear translocation, transactivation potential, and proteasome-
584 mediated degradation. Mol Cell Biol 18:2986-96.
585 43. Servant MJ, Grandvaux N, tenOever BR, Duguay D, Lin R, Hiscott J. 2003. Identification of the
586 minimal phosphoacceptor site required for in vivo activation of interferon regulatory factor 3 in
587 response to virus and double-stranded RNA. J Biol Chem 278:9441-7.
588 44. Chen W, Srinath H, Lam SS, Schiffer CA, Royer WE, Jr., Lin K. 2008. Contribution of Ser386 and
589 Ser396 to activation of interferon regulatory factor 3. Journal of molecular biology 379:251-260.
590 45. Hausmann Y, Roman-Sosa G, Thiel H-J, Rümenapf T. 2004. Classical swine fever virus
591 glycoprotein E rns is an endoribonuclease with an unusual base specificity. Journal of virology
592 78:5507-5512.
593 46. Lussi C, Sauter K-S, Schweizer M. 2018. Homodimerisation-independent cleavage of dsRNA by a
594 pestiviral nicking endoribonuclease. Scientific Reports 8:8226.
595 47. Baum A, Sachidanandam R, García-Sastre A. 2010. Preference of RIG-I for short viral RNA
596 molecules in infected cells revealed by next-generation sequencing. Proceedings of the National
597 Academy of Sciences of the United States of America 107:16303-16308.
598 48. Kato H, Takahasi K, Fujita T. 2011. RIG-I-like receptors: cytoplasmic sensors for non-self RNA.
599 Immunol Rev 243:91-8.
600 49. Strahle L, Garcin D, Kolakofsky D. 2006. Sendai virus defective-interfering genomes and the
601 activation of interferon-beta. Virology 351:101-11.
602 50. Shaw AE, Hughes J, Gu Q, Behdenna A, Singer JB, Dennis T, Orton RJ, Varela M, Gifford RJ,
603 Wilson SJ, Palmarini M. 2017. Fundamental properties of the mammalian innate immune system
604 revealed by multispecies comparison of type I interferon responses. PLOS Biology 15:e2004086.
605 51. Renson P, Blanchard Y, Le Dimna M, Felix H, Cariolet R, Jestin A, Le Potier M-FJVR. 2010. Acute
606 induction of cell death-related IFN stimulated genes (ISG) differentiates highly from moderately
607 virulent CSFV strains. 41:07.
608 52. Kaiser WJ, Kaufman JL, Offermann MK. 2004. IFN-alpha sensitizes human umbilical vein
609 endothelial cells to apoptosis induced by double-stranded RNA. J Immunol 172:1699-710.
610 53. Garcin D, Marq JB, Strahle L, le Mercier P, Kolakofsky D. 2002. All four Sendai Virus C proteins
611 bind Stat1, but only the larger forms also induce its mono-ubiquitination and degradation.
612 Virology 295:256-65.
613 54. Eskes R, Desagher S, Antonsson B, Martinou JC. 2000. Bid induces the oligomerization and
614 insertion of Bax into the outer mitochondrial membrane. Mol Cell Biol 20:929-35.
615 55. Subburaj Y, Cosentino K, Axmann M, Pedrueza-Villalmanzo E, Hermann E, Bleicken S, Spatz J,
616 Garcia-Saez AJ. 2015. Bax monomers form dimer units in the membrane that further self-
617 assemble into multiple oligomeric species. Nat Commun 6:8042.
618 56. Westphal D, Kluck RM, Dewson G. 2014. Building blocks of the apoptotic pore: how Bax and Bak
619 are activated and oligomerize during apoptosis. Cell Death & Differentiation 21:196-205.
620 57. Cosentino K, García-Sáez AJ. 2017. Bax and Bak Pores: Are We Closing the Circle? Trends in cell
621 biology 27:266-275.

622 58. Kuwana T, Mackey MR, Perkins G, Ellisman MH, Latterich M, Schneiter R, Green DR, Newmeyer
623 DD. 2002. Bid, Bax, and Lipids Cooperate to Form Supramolecular Openings in the Outer
624 Mitochondrial Membrane. Cell 111:331-342.
625 59. Zhang M, Zheng J, Nussinov R, Ma B. 2017. Release of Cytochrome C from Bax Pores at the
626 Mitochondrial Membrane. Scientific Reports 7:2635.
627 60. Jurgensmeier JM, Xie Z, Deveraux Q, Ellerby L, Bredesen D, Reed JC. 1998. Bax directly induces
628 release of cytochrome c from isolated mitochondria. Proc Natl Acad Sci U S A 95:4997-5002.
629 61. Jefferson M, Whelband M, Mohorianu I, Powell PP. 2014. The pestivirus N terminal protease
630 N(pro) redistributes to mitochondria and peroxisomes suggesting new sites for regulation of
631 IRF3 by N(pro.). PLoS One 9:e88838.
632 62. Lau ATY, Li M, Xie R, He Q-Y, Chiu J-F. 2004. Opposed arsenite-induced signaling pathways
633 promote cell proliferation or apoptosis in cultured lung cells. Carcinogenesis 25:21-28.
634 63. Hüsser L, Alves MP, Ruggli N, Summerfield A. 2011. Identification of the role of RIG-I, MDA-5 and
635 TLR3 in sensing RNA viruses in porcine epithelial cells using lentivirus-driven RNA interference.
636 Virus Research 159:9-16.
637 64. Bensaude E, Turner JL, Wakeley PR, Sweetman DA, Pardieu C, Drew TW, Wileman T, Powell PP.
638 2004. Classical swine fever virus induces proinflammatory cytokines and tissue factor expression
639 and inhibits apoptosis and interferon synthesis during the establishment of long-term infection
640 of porcine vascular endothelial cells. J Gen Virol 85:1029-37.
641 65. Sancak Y, Peterson TR, Shaul YD, Lindquist RA, Thoreen CC, Bar-Peled L, Sabatini DM. 2008. The
642 Rag GTPases bind raptor and mediate amino acid signaling to mTORC1. Science 320:1496-501.
643 66. Ran FA, Hsu PD, Wright J, Agarwala V, Scott DA, Zhang F. 2013. Genome engineering using the
644 CRISPR-Cas9 system. Nature Protocols 8:2281.
645 67. La Rocca SA, Herbert RJ, Crooke H, Drew TW, Wileman TE, Powell PP. 2005. Loss of interferon
646 regulatory factor 3 in cells infected with classical swine fever virus involves the N-terminal
647 protease, Npro. J Virol 79:7239-47.

648

649

650

651

652

653

654 **Figure 1**: N^{pro} antagonises poly(I:C) and Sendai virus-mediated apoptosis in PK-15 cells. (A) PK-15

655 cells or PK-15 cells stably expressing His-N^{pro}, or (B) PK-15 cells stably expressing EGFP (*) or

656 EGFP-N^{pro} (**) were seeded in 12-well plates and treated with poly(I:C) or SeV. 18 hours post-

657 treatment, whole cell lysates were prepared and analysed by Western blotting using polyclonal

658 Abs recognising ISG15, N^{pro} or GFP and mAbs recognising cleaved caspase-3, Mx1 or RIG-I as

659 indicated. (C) PK-15 cells, PK-15 cells stably expressing His-N^{pro} or PK-15 cells infected (MOI of
660 0.5) with CSFV Alfort for 24 hr were treated with STS. 8 hours post-treatment, whole cell lysates
661 were prepared and analysed by Western blotting using a polyclonal Ab recognising N^{pro} and a
662 mAb recognising cleaved caspase-3 as indicated. (A-C) A mAb recognising γ-tubulin was used to
663 determine relative protein concentrations. Experiments were repeated on at least two separate
664 occasions.

665 **Figure 2**: Type I IFN amplifies poly(I:C)-mediated apoptosis but is not essential for its induction.
666 (A) Schematic representation of RXT inhibition of JAK/STAT-mediated IFN response. (B) PK-15
667 cells were seeded in 12-well plates and treated with poly(I:C) or SeV in the presence or absence
668 of JAK-STAT inhibitor RXT. 18 hours post-treatment, whole cell lysates were prepared and
669 analysed by Western blot using a polyclonal Ab recognising ISG15 or mAbs recognising cleaved
670 caspase-3, Mx1, RIG-I, or GFP as indicated. A mAb recognising γ-tubulin was used to determine
671 relative protein concentrations. (C) PK-15 and SK6 cells were seeded in 12-well plates and
672 treated with increasing concentrations of porcine IFN-α in the presence or absence of poly(I:C).
673 18 hours post-treatment, whole cell lysates were prepared and analysed by Western blot as in
674 (A). Experiments were repeated on at least two separate occasions.

675 **Figure 3**: Poly(I:C) and SeV induce apoptosis through TLR3/IRF3 and RIG-I/IRF3 signalling
676 pathways, respectively. (A-F) WT PK-15 and knockout PK-15 cell lines ($TLR3^{-/-}$, $RIG\text{-}I^{-/-}$, $IRF3^{-/-}$)
677 were seeded in 12-well plates and treated with poly(I:C) (A, C, E) or SeV (B, D, F) in the presence
678 or absence of RXT. 18 hours post-treatment, whole cell lysates were harvested and analysed by
679 Western blot using a polyclonal Ab recognising ISG15 and mAbs recognising cleaved caspase-3,

680 Mx1, or RIG-I as indicated. A mAb recognising γ-tubulin was used to determine relative protein
681 concentrations. Experiments were repeated on at least two separate occasions.

682 **Figure 4:** Bax directly mediates apoptosis in a manner that relies upon transcription-
683 independent functions of IRF3**.** (A) Yeast co-transformed with plasmids expressing the indicated
684 proteins fused to either the GAL4 DNA-binding domain (in pGBKT7) or activation domain (in
685 pGADT7) were cultured on dropout media to identify interactions. Co-transfection of plasmids
686 encoding N^{pro}, BaxΔC or IRF3 with the reciprocal plasmid vector (pGBKT7 or pGADT7) served as
687 negative interaction controls. Co-transfection of the large T antigen (T) and p53 or T and Lamin
688 served as positive and negative system controls. (B, C) WT and $Bax^{-/-}$ PK-15 cell lines were
689 seeded in 12-well plates and treated with poly(I:C) or SeV. 18 hours post-treatment, whole cell
690 lysates were (B) imaged, (C) harvested and analysed by Western blot using polyclonal Abs
691 recognising ISG15 or Bax and mAbs recognising cleaved caspase-3 or Mx1. (D) Alignments of
692 porcine, human and murine IRF3 protein sequences implicated in transcriptional activity
693 (turquoise) were performed in MEGA7. Mutations (pink) were designed in porcine IRF3 (poIRF3)
694 to generate N-terminal FLAG-tagged WT and S1 mutant (S394A, S396A) poIRF3 fusion proteins.
695 Conserved (*) and non-conserved residues (-) are indicated. (E) Pools of $IRF3^{-/-}$ PK-15 cells
696 expressing WT or S1 mutant FLAG-tagged IRF3 were prepared and treated as previously
697 detailed (B, C). Western blot analysis was performed using a polyclonal Ab recognising the FLAG
698 epitope (DYKDDDDK) and mAbs recognising cleaved caspase-3 or Mx1. (C, E) A mAb recognising
699 γ-tubulin was used to determine relative protein concentrations. Experiments were repeated on
700 at least two separate occasions.

701 **Figure 5**: N^{pro} blocks poly(I:C) and Sendai virus-mediated mitochondrial localisation of pro-
702 apoptotic Bax. (A) WT, $IRF3^{-/-}$ and His-N^{pro}-expressing PK-15 cells were treated with poly(I:C) or
703 SeV in the presence of 100 µM caspase inhibitor Z-VAD(OMe)-FMK (Bachem). 18 hours post-
704 treatment, cells were treated with Mitotracker and analysed by immunofluorescence using a
705 polyclonal Ab recognising Bax. Nuclei are stained blue with DAPI. Scale bars represent 45 µM.
706 (B) Immunofluorescence images of single cells were collected from the experiment detailed in
707 (A). Scale bars represent 20 µM. (C, D) Whole cell lysates prepared from replicate samples of (A)
708 were analysed by Western blot using polyclonal Abs recognising Bax or N^{pro} and a mAb
709 recognising cleaved caspase-3. A mAb recognising γ-tubulin was used to determine relative
710 protein concentrations. Experiments were repeated on at least two separate occasions.

711 **Figure 6**: Antagonism of SeV-mediated apoptosis in CSFV-infected cells is dependent on the
712 expression of N^{pro}. (A) WT PK-15 and SK6 cells were infected (MOI of 0.2) with CSFV Alfort, CSFV
713 Brescia, rCSFV Alfort or ΔN^{pro} rCSFV Alfort as indicated for 72 hr and then treated with SeV. 18
714 hours post-treatment, cells were treated with Mitotracker and analysed by immunofluorescence
715 staining using a polyclonal Ab recognising Bax and a mAb recognising CSFV E2. Nuclei are
716 stained blue with DAPI. (B, C) The percentage of cells displaying Bax localisation to the
717 mitochondria following each treatment was then quantified; ***: $p<.001$. Experiments were
718 repeated on at least two separate occasions.

719 **Figure 7**: Model of TLR3 and RIG-I-mediated apoptosis and its antagonism by CSFV N^{pro}. Upon
720 stimulation with poly(I:C) and SeV, TLR3 and RIG-I initiate apoptosis in an IRF3-dependent
721 manner, independent of its functions as a transcription factor and characterised by
722 mitochondrial relocalisation of Bax and activation of caspase-3. IRF3 also triggers induction of

723 IFN-β and IFN-dependent and independent upregulation of ISGs which might amplify the

724 TLR3/IRF3 signalling axis. CSFV N^{pro} (purple), apoptotic signalling (red), IFN signalling (blue) and

725 uncertain or inferred pathways (?) are indicated.

726 **Table 1**: Cas9 target sequences within the coding sequence of each gene and their respective

727 offsets.

728

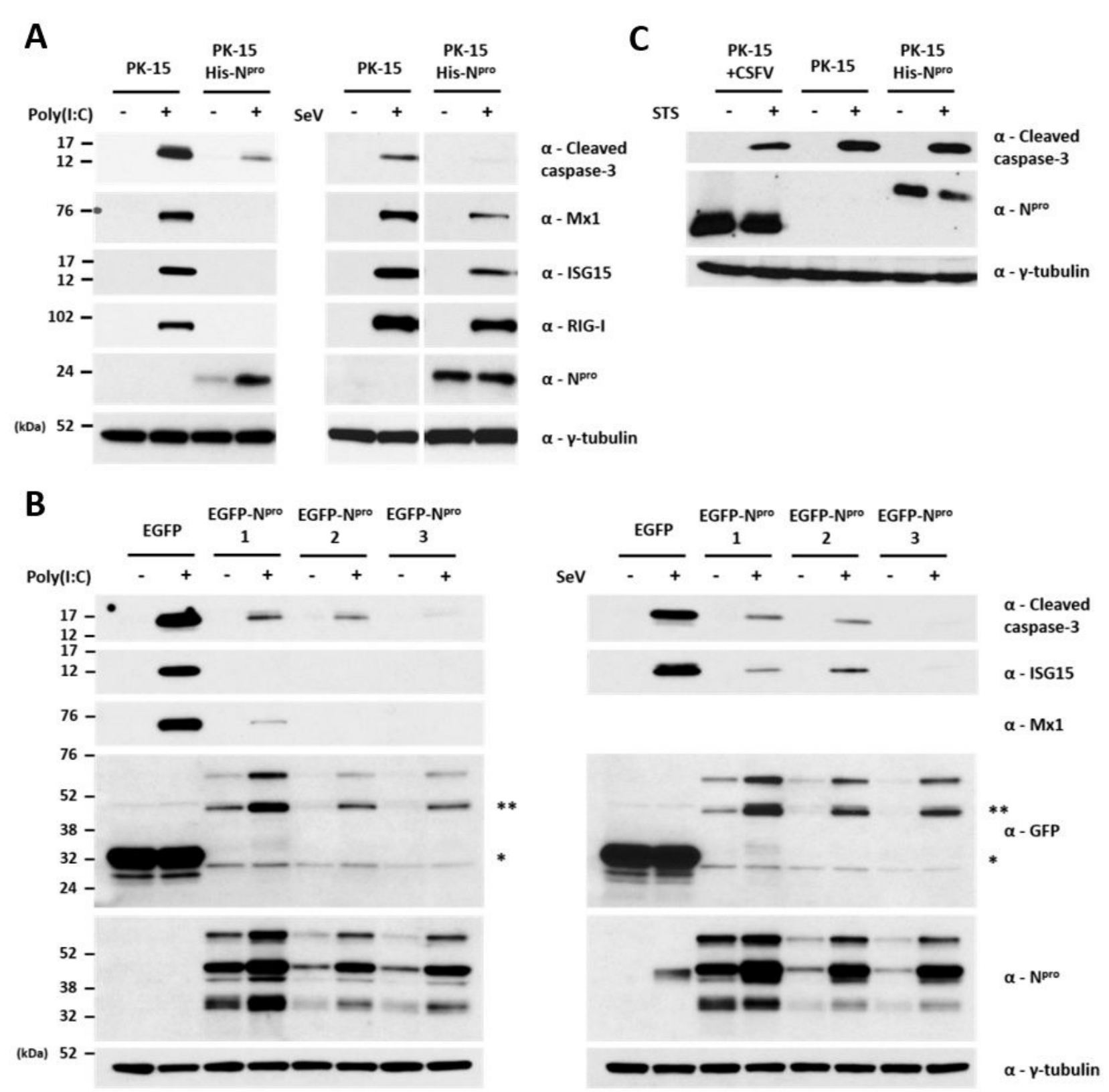
A
PK-15
PK-15 His-Npro
Poly(I:C)
SeV
17
12
76
102
24
52
(kDa)
α - Cleaved caspase-3
α - Mx1
α - ISG15
α - RIG-I
α - Npro
α - γ-tubulin
C
PK-15 +CSFV
PK-15
PK-15 His-Npro
STS
α - Cleaved caspase-3
α - Npro
α - γ-tubulin
B
EGFP
EGFP-Npro 1
EGFP-Npro 2
EGFP-Npro 3
Poly(I:C)
SeV
17
12
76
52
38
32
24
(kDa)
**
*
α - Cleaved caspase-3
α - ISG15
α - Mx1
α - GFP
α - Npro
α - γ-tubulin

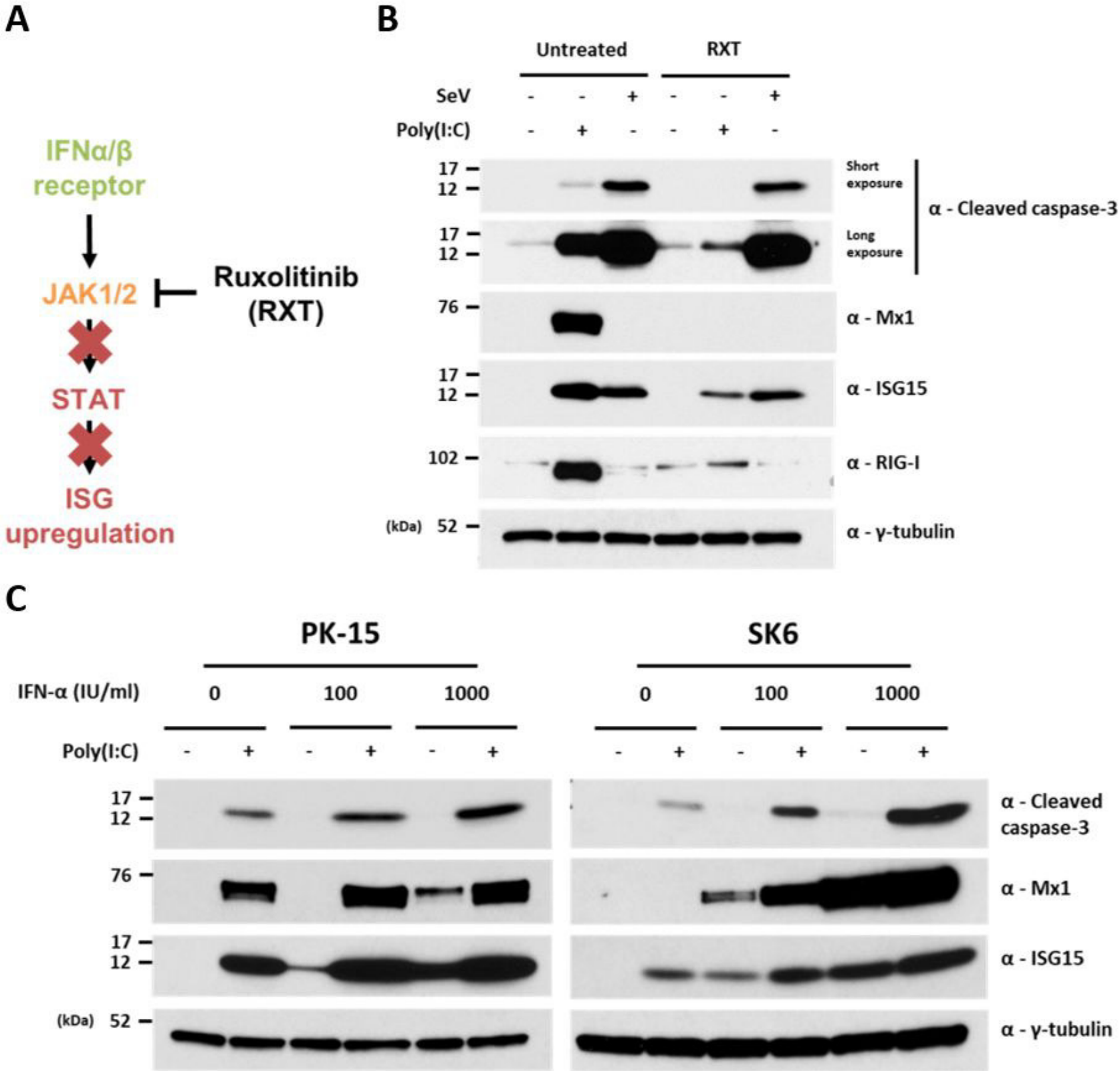
A
IFNα/β receptor
JAK1/2
Ruxolitinib (RXT)
STAT
ISG upregulation
B
Untreated
RXT
SeV
Poly(I:C)
17
12
76
102
52
(kDa)
Short exposure
Long exposure
α - Cleaved caspase-3
α - Mx1
α - ISG15
α - RIG-I
α - γ-tubulin
C
PK-15
SK6
IFN-α (IU/ml)
0
100
1000
Poly(I:C)
α - Cleaved caspase-3
α - Mx1
α - ISG15
α - γ-tubulin

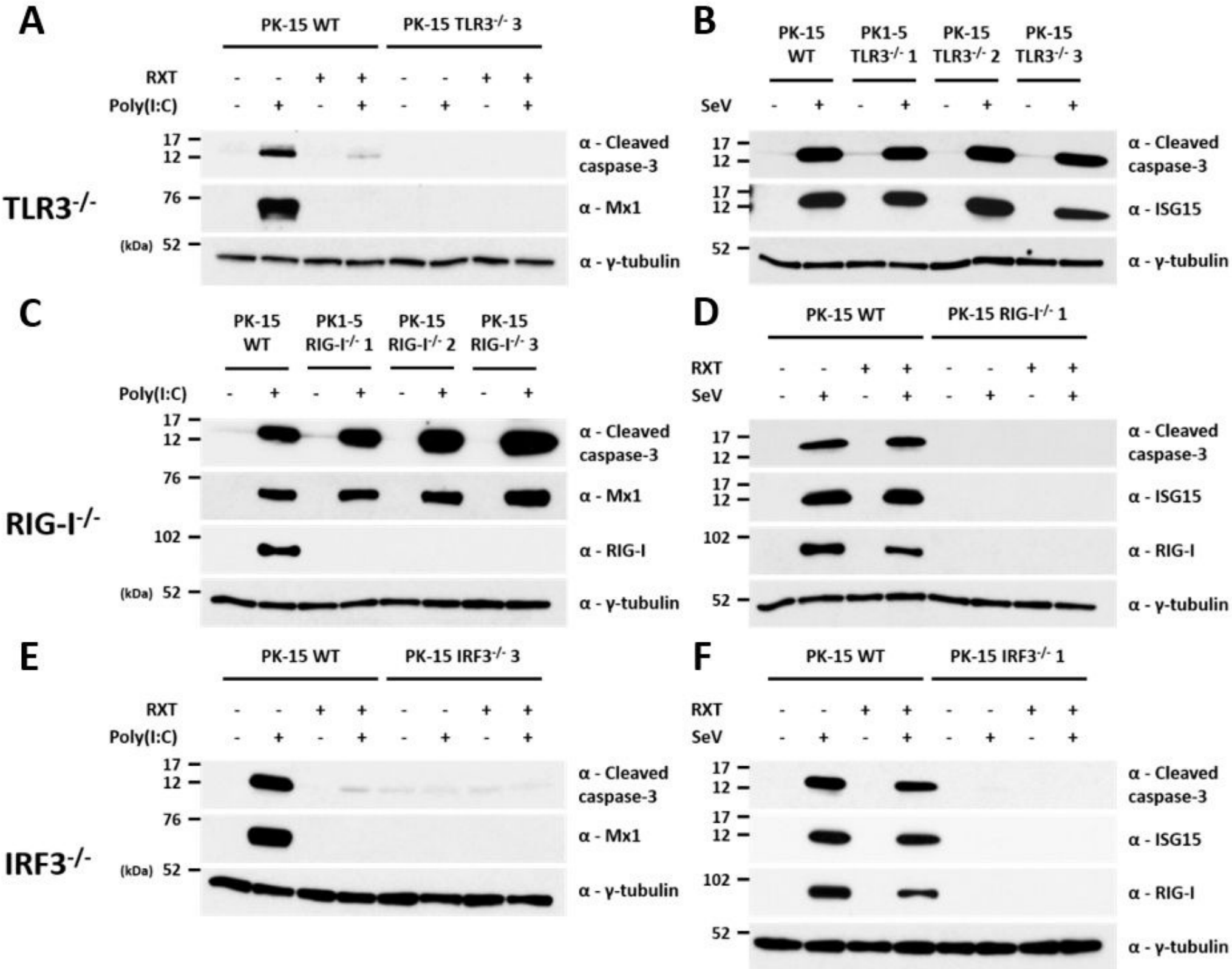
A
PK-15 WT
PK-15 TLR3-/- 3
RXT
Poly(I:C)
TLR3-/-
17
12
76
52
(kDa)
α - Cleaved caspase-3
α - Mx1
α - γ-tubulin
B
PK-15 WT
PK1-5 TLR3-/- 1
PK-15 TLR3-/- 2
PK-15 TLR3-/- 3
SeV
α - ISG15
C
PK-15 WT
PK1-5 RIG-I-/- 1
PK-15 RIG-I-/- 2
PK-15 RIG-I-/- 3
RIG-I-/-
102
α - RIG-I
D
PK-15 WT
PK-15 RIG-I-/- 1
E
PK-15 WT
PK-15 IRF3-/- 3
IRF3-/-
F
PK-15 WT
PK-15 IRF3-/- 1

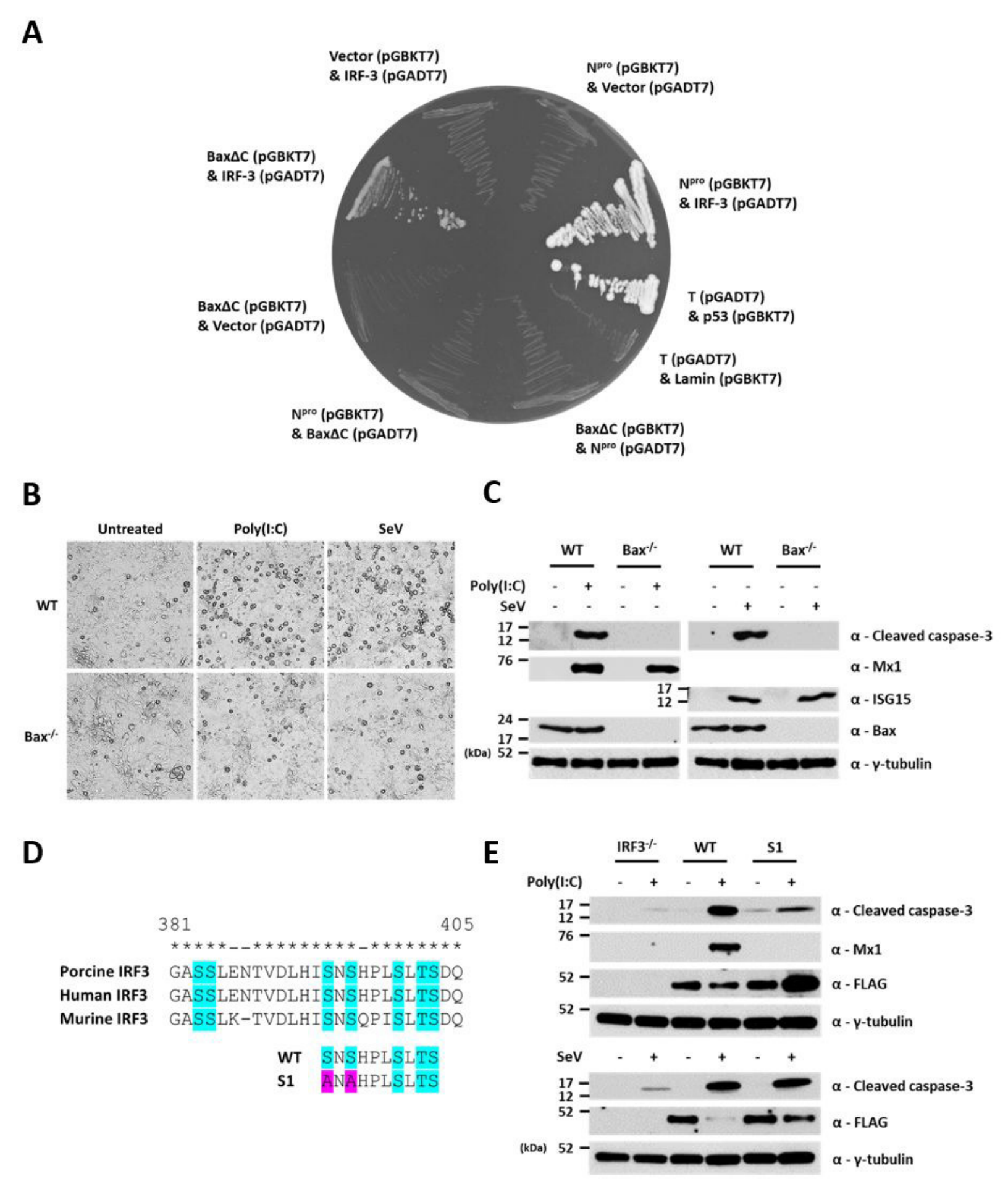
A
Vector (pGBKT7)
& IRF-3 (pGADT7)
Npro (pGBKT7)
& Vector (pGADT7)
BaxΔC (pGBKT7)
& IRF-3 (pGADT7)
Npro (pGBKT7)
& IRF-3 (pGADT7)
BaxΔC (pGBKT7)
& Vector (pGADT7)
T (pGADT7)
& p53 (pGBKT7)
T (pGADT7)
& Lamin (pGBKT7)
Npro (pGBKT7)
& BaxΔC (pGADT7)
BaxΔC (pGBKT7)
& Npro (pGADT7)
B
Untreated
Poly(I:C)
SeV
WT
Bax-/-
C
WT
Bax-/-
WT
Bax-/-
Poly(I:C)
SeV
17
12
76
24
17
(kDa) 52
α - Cleaved caspase-3
α - Mx1
α - ISG15
α - Bax
α - γ-tubulin
D
381
405
Porcine IRF3 GASSLENTVDLHISNSHPLSLTSDQ
Human IRF3 GASSLENTVDLHISNSHPLSLTSDQ
Murine IRF3 GASSLK-TVDLHISNSQPISLTSDQ
WT SNSHPLSLTS
S1 ANAHPLSLTS
E
IRF3-/-
WT
S1
Poly(I:C)
17
12
76
52
52
α - Cleaved caspase-3
α - Mx1
α - FLAG
α - γ-tubulin
SeV
17
12
52
(kDa) 52
α - Cleaved caspase-3
α - FLAG
α - γ-tubulin

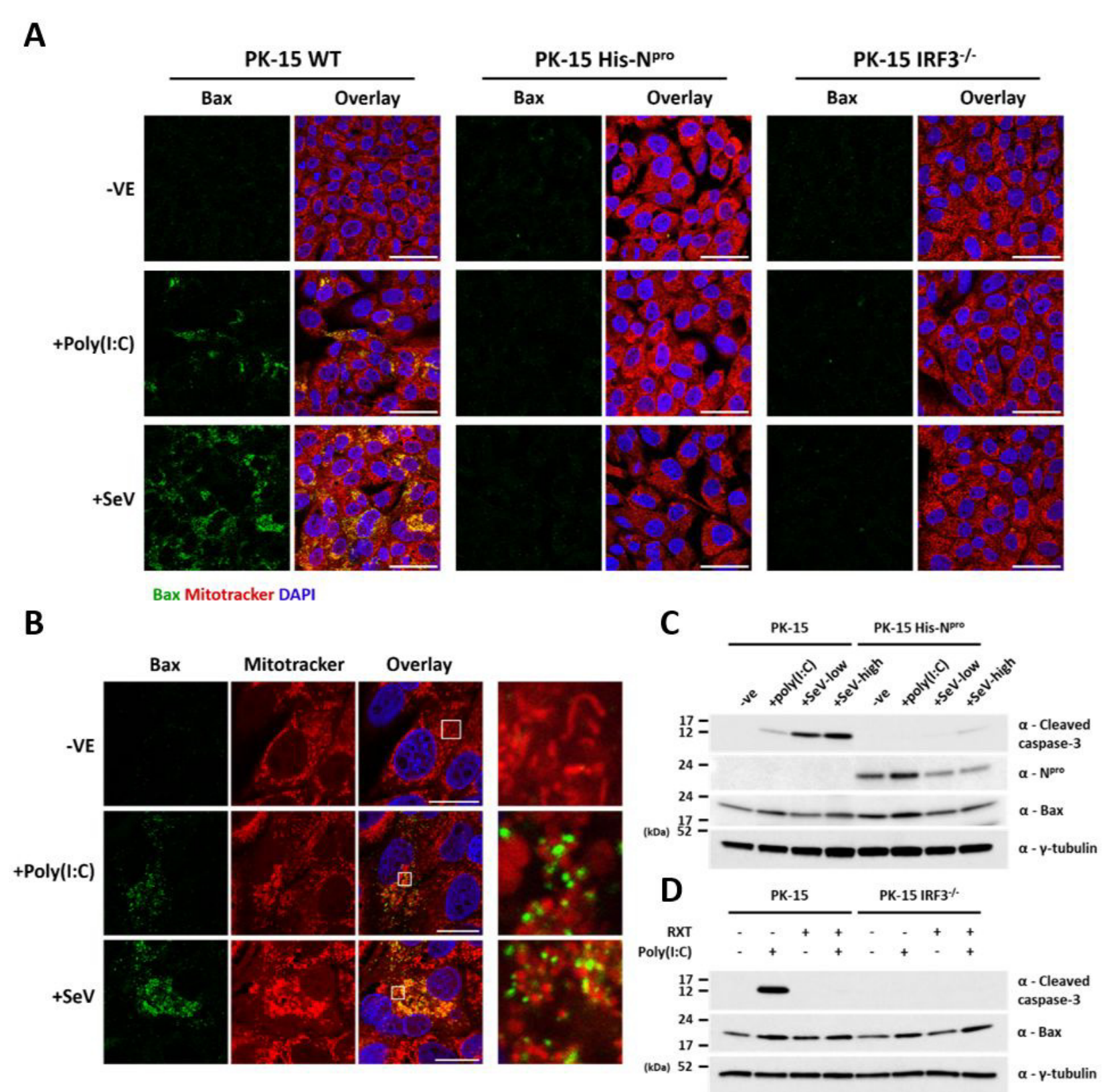
A
PK-15 WT
PK-15 His-Npro
PK-15 IRF3-/-
Bax
Overlay
-VE
+Poly(I:C)
+SeV
Bax Mitotracker DAPI
B
Bax
Mitotracker
Overlay
-VE
+Poly(I:C)
+SeV
C
PK-15
PK-15 His-Npro
-ve
+poly(I:C)
+SeV-low
+SeV-high
17
12
24
24
17
(kDa) 52
α - Cleaved caspase-3
α - Npro
α - Bax
α - γ-tubulin
D
PK-15
PK-15 IRF3-/-
RXT
Poly(I:C)
17
12
24
17
(kDa) 52
α - Cleaved caspase-3
α - Bax
α - γ-tubulin

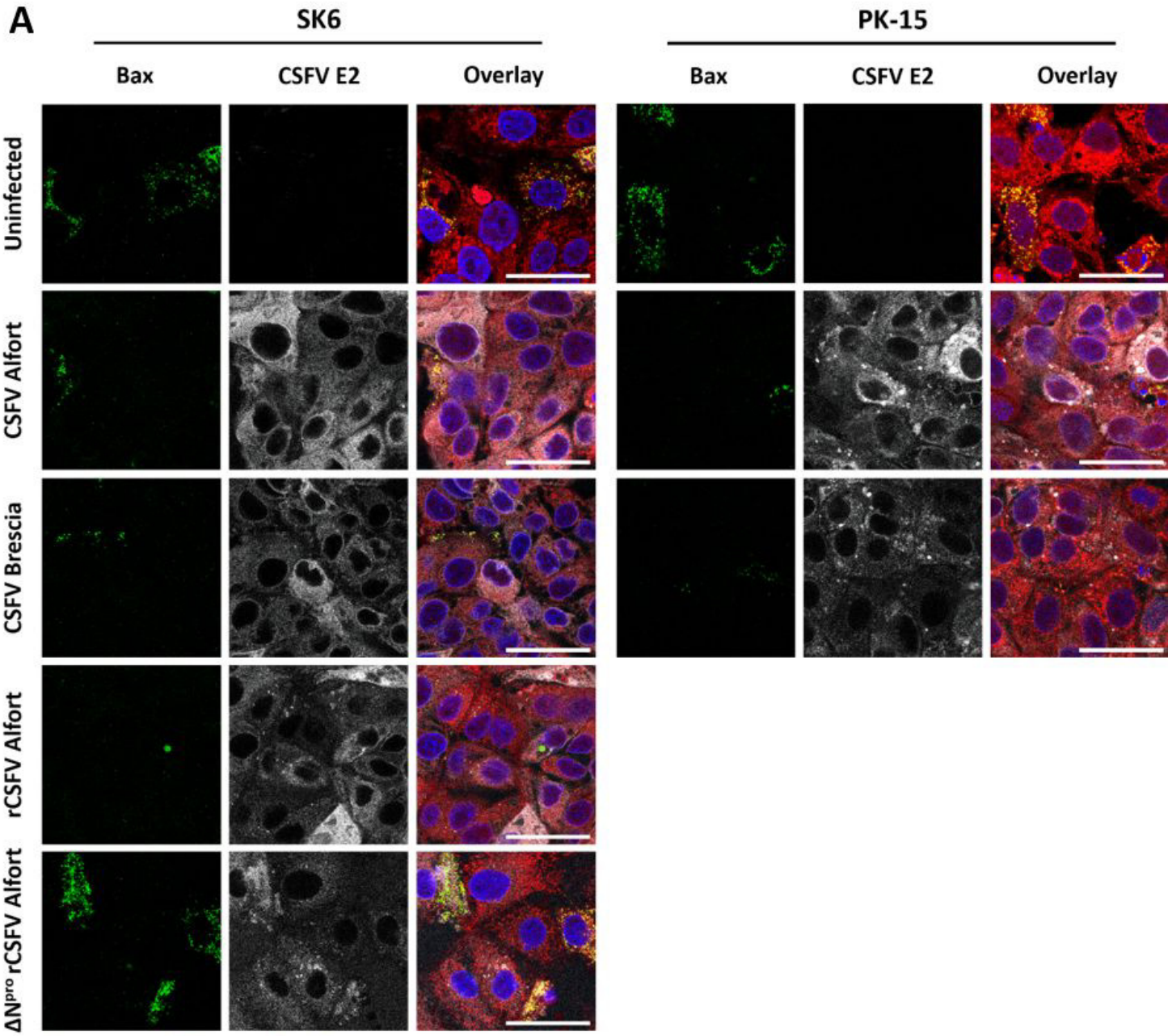
A
SK6
PK-15
Bax
CSFV E2
Overlay
Uninfected
CSFV Alfort
CSFV Brescia
rCSFV Alfort
ΔN^pro rCSFV Alfort
Bax CSFV E2 Mitotracker DAPI

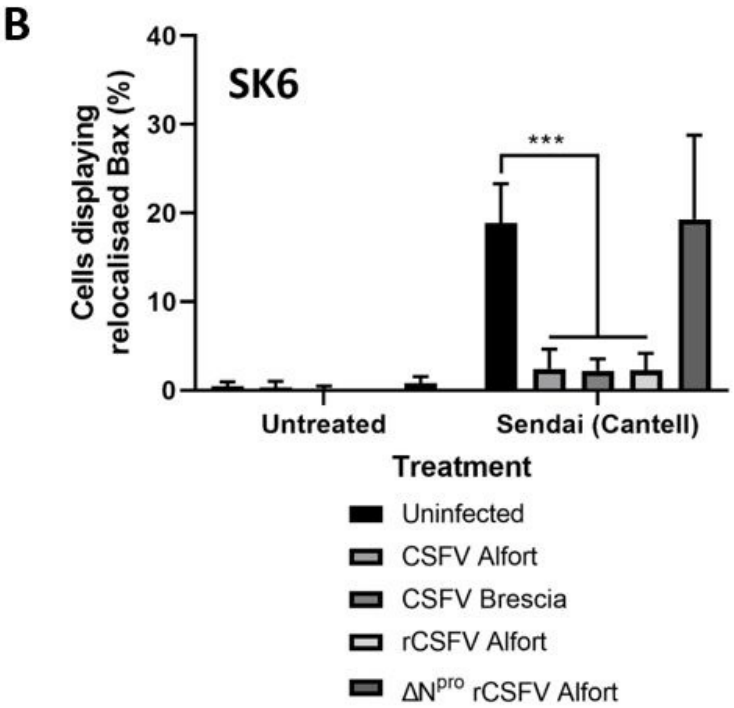
B
SK6
Cells displaying relocalisaed Bax (%)
40
30
20
10
0
***
Untreated
Sendai (Cantell)
Treatment
Uninfected
CSFV Alfort
CSFV Brescia
rCSFV Alfort
ΔN^pro rCSFV Alfort

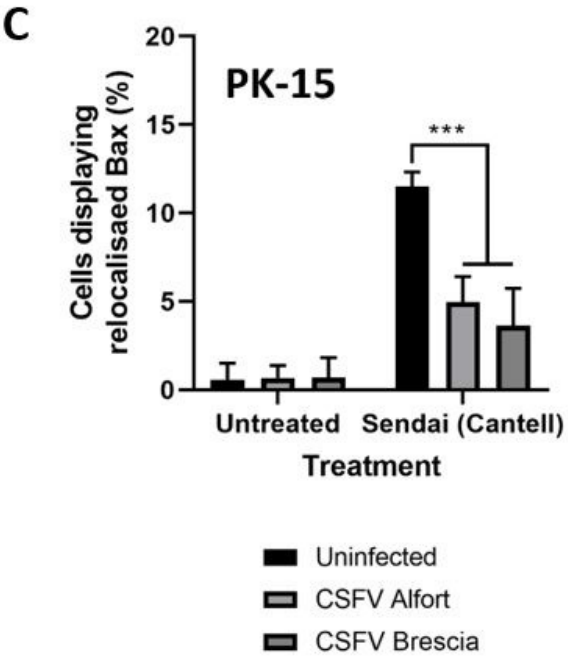
C
PK-15
Cells displaying relocalisaed Bax (%)
20
15
10
5
0
***
Untreated
Sendai (Cantell)
Treatment
Uninfected
CSFV Alfort
CSFV Brescia

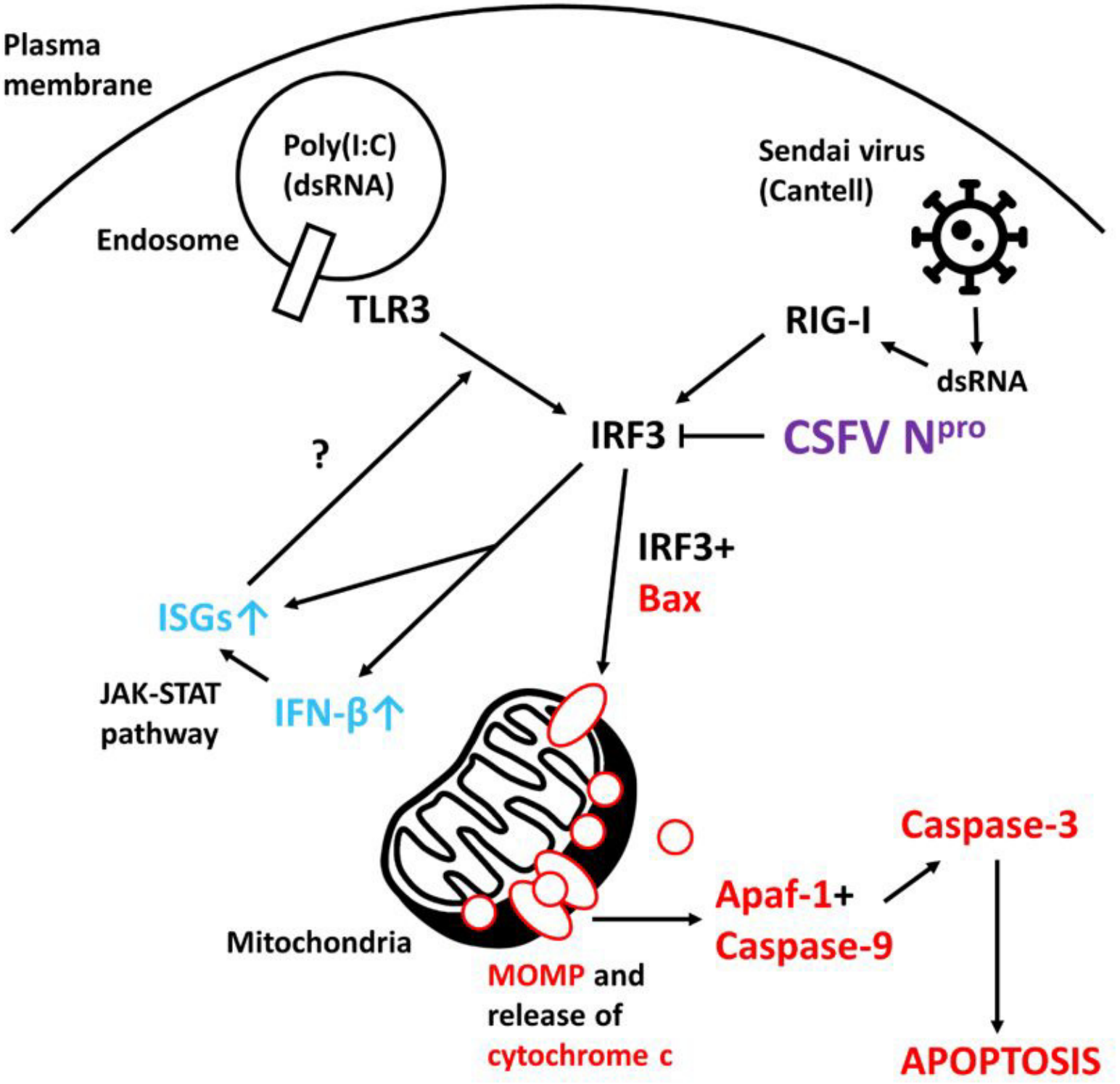
Plasma membrane
Poly(I:C) (dsRNA)
Endosome
TLR3
Sendai virus (Cantell)
RIG-I
dsRNA
IRF3
CSFV Npro
?
IRF3+ Bax
ISGs↑
JAK-STAT pathway
IFN-β↑
Mitochondria
MOMP and release of cytochrome c
Apaf-1+ Caspase-9
Caspase-3
APOPTOSIS

Knock-out target	sgRNA-1 (px461)	sgRNA-2 (px462)	Offset
IRF3	GCCGCAAGCCGTGCTTCCAA	GGAGGACTTCGGCATCTTCC	+13
TLR3	CTCCATCCAAGGTAGTAAGT	ATTTAACACCATCTCAAAGC	+1
RIG-I	GATGATGGAGATAGAGAGTC	GATGCACTTAAATCTGTCAG	+11
Bax	TTCTTGGTAGATGCATCCTG	AGCGAGTGTCTCAAGCGCAT	+4